Mathematical Modelling and Analysis
Volume 14 Number 4, 2009, pages 515–529
Doi:10.3846/1392-6292.2009.14.515-529

ISSN 1392-6292 print
ISSN 1648-3510 online
www.vgtu.lt/mma/

On Taylor's Scraping Problem and Flow of a Sisko Fluid

A. M. Siddiqui[1], A. R. Ansari[2], A. Ahmad[3] and N. Ahmad[4] (late)

[1] *Pennsylvania State University*
Department of Mathematics, York Campus, York, PA 17403, USA
[2] *Gulf University for Science & Technology*
Department of Mathematics & Natural Sciences, P.O. Box 7207, Hawally 32093, Kuwait
[3] *Quaid-i-Azam University*
[3,4]Department of Mathematics, Islamabad, Pakistan.
E-mail(*corresp.*): ansari.a@gust.edu.kw
E-mail: ams5@psu.edu

Received April 1, 2009; revised July 16, 2009; published online November 10, 2009

Abstract. The aim of the present investigation is to study the properties of a Sisko fluid flowing between two intersecting planes. The problem is similar to Taylor's scraping problem for a viscous fluid. We determine the solution of the complicated set of non-linear partial differential equations describing the flow analytically. The analysis is carried out in detail reflecting the effects of varying the angle of the scraper on the flow. In addition, the tangential and normal stress are also computed. We also show the well known Taylor scraper problem as a special case.

Key words: non-newtonian fluid model, Sisko fluid, homotopy perturbation method.

1 Introduction

Non-Newtonian fluid models have been the source of considerable interest to researchers in the last two decades. In particular, this work focuses on the model of non-Newtonian fluids proposed by Sisko [23]. Many real fluids follow the Sisko model. Polymeric suspensions such as waterborne coatings are known to be non-Newtonian in nature and are known to follow the Sisko model [25]. The viscosity of such coatings depends on the shear rate and the strain history. An example that lends itself to such types of coating is metallic automotive basecoat. Of course the most well know Sisko fluids are lubricating greases [23]. In fact most psueodplastic fluids, drilling fluids and cement slurries without

yield stress follow the Sisko model [8]. In [2] it is shown that the Sisko model is one of the best of 11 models analyzed for non-Newtonian fluids.

The dynamics of scraping of non-Newtonian fluids has many applications in the food industry, such as cleaning of pipes that conduit fluids used in the processing of various foods. The mathematical model representing the dynamics of scraping of a viscous fluid was originally proposed by Taylor, better known as the Taylor scraper [24]. The geometry of the flow of interest here has been studied by several other authors. For instance, Stokes flow between two intersecting planes was studied by Moffat [19]. The creeping corner flow induced by a steady in-plane motion of the walls was later examined by Batchelor [3], but the investigations were restricted to Newtonian fluids. Mansutti and Rajagopal [17] studied the non-inertial flow of a shear thinning fluid between intersecting planes. They showed that sharp and pronounced boundary layers develop adjacent to the solid boundaries, even at zero Reynolds number. In addition, Bhatnagar *et al.* [4] have extended the analysis to an Oldroyd-B fluid.

In the case of most non-Newtonian fluids a purely radial flow is not possible if the inertial terms are to be retained in the equations of motion. Kaloni and Kamel [12] have shown that there cannot be a purely radial flow of Cosserat fluids in convergent channels. Later, Hull [11] studied the non-inertial flow of a general linear viscoelastic fluid with this geometry. He have shown that radial flow is obtained for a wedge of 90° and no others. In addition, similar results are valid for the Rivlin-Ericksen fluids. Further recent work on non-Newtonian fluids can be found in [13].

Our objective in this paper is to consider a model which tries to depict the scraping of a Sisko fluid such as waterborne paint or grease. There are many possible applications of such models. For instance in scraping certain wet paints, also in the scraping of cement slurries. In addition, scraping of drilling fluids from pipes can also be considered. Having described the problem and a short history of the work we now turn our attention to the method of solution. Until recently, nonlinear analytical techniques for solving nonlinear problems have been dominated by the perturbation methods, which have found wide applications in engineering [14, 15, 16, 20]. But, like other nonlinear analytical techniques, perturbation methods have their own limitations. The main restriction is that almost all perturbations are based on small parameters so that the approximate solution can be expressed in a series of small parameters. This so called small parameter assumption greatly restricts application of perturbation techniques, as it is well known, an overwhelming majority of nonlinear problems have no small parameters at all. The restrictions in traditional perturbation methods, have been addressed in [9, 10], who gave a heuristical method based on the homotopy in topology. The method offers alternatives that overcome the restrictions posed by traditional perturbation methods. On the other hand it can take full advantage of the classical perturbation techniques so there has been a considerable amount of research in applying HPM for solving various strongly nonlinear equations. For instance Abbasbandy [1] have used it for the Laplace transforms, Cveticanin [6] applied it to study pure nonlinear differential equations and El-Shahed [7] applied this technique to the integro-differential equation for Voltera's model. In addition, Siddiqui

et al. [21, 22] have recently applied this method to analyze flow problems in non-Newtonian fluid mechanics. We also note that Homotopy Perturbation Method is a member of a class of perturbation methods that are independent of the small parameter restriction, other methods include the Optimal Homotopy Analysis Method and the Variational Iteration Method [18].

In summary, in this paper, we consider the flow of a non-Newtonian fluid between two rigid boundaries forming a wedge, the problem is similar to one proposed by Taylor [24]. The fluid under consideration is assumed to obey the model proposed by Sisko [23]. The problem is formulated in the following sections, and is solved by using the Homotopy Perturbation Method. By setting certain parameters we verify that the solutions take a form similar to [24].

2 Basic Equations

We start with the general constitutive equation of an incompressible Sisko fluid which is given as

$$\mathbf{T} = -p\mathbf{I} + a\mathbf{A}_1 + b\left(\mathrm{tr}\mathbf{A}_1^2\right)^m \mathbf{A}_1 = -p\mathbf{I} + \mathbf{S},$$

where $\mathbf{S} = \sum_{i=1}^{2} \mathbf{S}_i$ with

$$\mathbf{S}_1 = a\mathbf{A}_1, \mathbf{S}_2 = b\left(\mathrm{tr}\mathbf{A}_1^2\right)^m \mathbf{A}_1,$$

p is the pressure and the coefficients a, b are material constants. For steady motion the Rivlin-Ericksen tensors satisfy the recursion relation

$$\mathbf{A}_{\Gamma+1} = (\mathrm{grad}\mathbf{A}_\Gamma)\,\mathbf{V} + \mathbf{A}_\Gamma \mathrm{grad}\mathbf{V} + (\mathbf{A}_\Gamma \mathrm{grad}\mathbf{V})^{\mathrm{T}}, \quad \mathbf{A}_0 = \mathbf{I}. \tag{2.1}$$

For a steady motion the field equations are given by:

$$\begin{aligned} &\mathrm{div}\mathbf{V}=0, \\ &\rho\,(\mathrm{grad}\mathbf{V})\,\mathbf{V} = -\mathrm{grad}p + \mathrm{div}\mathbf{S}, \end{aligned} \tag{2.2}$$

where ρ is the constant density; the body force in this case is negligible.

3 Problem Statement and the Equations of Motion

We consider two rigid planes in contact with each other having a constant inclination θ_0. We assume that one plane is sliding over the other with constant velocity U, we call the plane tilted at angle $\theta = \theta_0$, the scraper, and the horizontal moving boundary, a plate. The situation is depicted in Fig. 1.

We propose that the Sisko fluid is in between the planes and flows due to the steady motion of one of the planes. For two dimensional flow, we will employ polar coordinates (r, θ). The boundary conditions are

$$\mathbf{V} = U\mathbf{e}_r \ \text{ at } \ \theta = 0, \quad \mathbf{V} = 0 \ \text{ at } \ \theta = \theta_0. \tag{3.1}$$

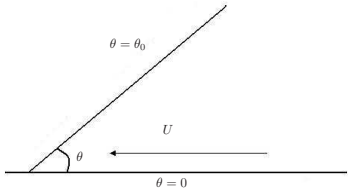

Figure 1. Two rigid planes intersecting at a fixed angle θ_0.

We assume that the velocity field and the pressure field in the fluid domain $(0 < \theta < \theta_0)$ are of the form

$$\mathbf{V}{=}u\,(r,\,\theta)\,\mathbf{e}_r + v\,(r,\,\theta)\,\mathbf{e}_\theta, \quad p = p\,(r,\,\theta)\,.$$

It is well known that for corner flows, the inertia forces are almost negligible and hence the field equation (2.2) reduces to

$$\mathrm{div}\mathbf{S} = \mathrm{grad}p. \tag{3.2}$$

Writing (3.2) in a component form [5], we have

$$\frac{\partial p}{\partial r} = -\frac{a}{r}\frac{\partial \Omega}{\partial \theta} + \frac{2b}{r}\frac{\partial}{\partial r}\Big(rM^m\frac{\partial u}{\partial r}\Big) + \frac{b}{r}\frac{\partial}{\partial \theta}\Big\{\Big(M^m\Big)\Big(\frac{1}{r}\frac{\partial u}{\partial \theta} + \frac{\partial v}{\partial r} - \frac{v}{r}\Big)\Big\}$$
$$- \frac{2b}{r}\Big\{\Big(M^m\Big)\Big(\frac{1}{r}\frac{\partial v}{\partial \theta} + \frac{u}{r}\Big)\Big\}, \tag{3.3}$$

and

$$\frac{1}{r}\frac{\partial p}{\partial \theta} = a\frac{\partial \Omega}{\partial r} + \frac{b}{r^2}\frac{\partial}{\partial r}r^2\Big\{M^m\Big(\frac{1}{r}\frac{\partial u}{\partial \theta} + \frac{\partial v}{\partial r} - \frac{v}{r}\Big)\Big\} + \frac{2b}{r}\frac{\partial}{\partial \theta}\Big\{M^m\Big(\frac{1}{r}\frac{\partial v}{\partial \theta} + \frac{u}{r}\Big)\Big\}, \tag{3.4}$$

where

$$M = 4\left(\frac{\partial u}{\partial r}\right)^2 + 4\left(\frac{1}{r}\frac{\partial v}{\partial \theta} + \frac{u}{r}\right)^2 + 2\left(\frac{1}{r}\frac{\partial u}{\partial \theta} + \frac{\partial v}{\partial r} - \frac{v}{r}\right)^2,$$
$$\Omega = \frac{\partial v}{\partial r} + \frac{v}{r} - \frac{1}{r}\frac{\partial u}{\partial \theta}.$$

Eliminating the pressure from (3.3) and (3.4) and then introducing the stream function $\psi\,(r, \theta)$ such that

$$u = \frac{1}{r}\frac{\partial \psi}{\partial \theta}, \quad v = -\frac{\partial \psi}{\partial r}, \tag{3.5}$$

we end up with

$$ar\nabla^4\psi = \frac{2b}{r}\frac{\partial^2}{\partial \theta \partial r}\Big\{r\Psi^m\Big(\frac{1}{r}\frac{\partial^2 \psi}{\partial \theta \partial r} - \frac{1}{r^2}\frac{\partial \psi}{\partial \theta}\Big)\Big\} \tag{3.6}$$
$$+ \frac{b}{r}\frac{\partial^2}{\partial \theta^2}\Big\{\Psi^m\Big(\frac{1}{r^2}\frac{\partial^2 \psi}{\partial \theta^2} - \frac{\partial^2 \psi}{\partial r^2} + \frac{1}{r}\frac{\partial \psi}{\partial r}\Big)\Big\}$$

$$+\frac{2b}{r}\frac{\partial}{\partial\theta}\Big\{\Psi^m\Big(\frac{1}{r}\frac{\partial^2\psi}{\partial\theta\partial r}-\frac{1}{r^2}\frac{\partial\psi}{\partial\theta}\Big)\Big\}-\frac{b}{r}\frac{\partial^2}{\partial r^2}\Big\{r^2\Psi^m\Big(\frac{1}{r^2}\frac{\partial^2\psi}{\partial\theta^2}-\frac{\partial^2\psi}{\partial r^2}+\frac{1}{r}\frac{\partial\psi}{\partial r}\Big)\Big\}$$
$$+\frac{b}{r^2}\frac{\partial^2}{\partial r^2}\Big\{r^2\Psi^m\Big(\frac{1}{r^2}\frac{\partial^2\psi}{\partial\theta^2}-\frac{\partial^2\psi}{\partial r^2}+\frac{1}{r}\frac{\partial\psi}{\partial r}\Big)\Big\}+2b\frac{\partial^2}{\partial\theta\partial r}\Big\{\Psi^m\Big(\frac{1}{r}\frac{\partial^2\psi}{\partial\theta\partial r}-\frac{1}{r^2}\frac{\partial\psi}{\partial\theta}\Big)\Big\},$$

where

$$\Psi=8\Big(\frac{1}{r}\frac{\partial^2\psi}{\partial\theta\partial r}-\frac{1}{r^2}\frac{\partial\psi}{\partial\theta}\Big)^2+2\Big(\frac{1}{r^2}\frac{\partial^2\psi}{\partial\theta^2}-\frac{\partial^2\psi}{\partial r^2}+\frac{1}{r}\frac{\partial\psi}{\partial r}\Big)^2,$$

the boundary conditions in terms of $\psi(r,\theta)$ are:

$$\frac{1}{r}\frac{\partial\psi}{\partial\theta}=U,\quad \frac{\partial\psi}{\partial r}=0\quad \text{at}\quad \theta=0,$$
$$\frac{1}{r}\frac{\partial\psi}{\partial\theta}=0,\quad \frac{\partial\psi}{\partial r}=0\quad \text{at}\quad \theta=\theta_0.$$

4 Solution of the Problem

The homotopy perturbation is a combination of classical perturbation technique and homotopy technique, by this technique we construct the homotopy [9];

$$h\left(\widetilde{\psi},q\right)=L\left(\widetilde{\psi}\right)-L\left(\psi_0\right)+qL\left(\psi_0\right)+q\left\{N\left(\widetilde{\psi}\right)-f\left(r,\theta\right)\right\}=0, \tag{4.1}$$

where $q\in[0,1]$ is an embedding parameter, and $\psi_0(r,\theta)$ is an initial guess approximation of (3.6). In addition, L,N are respectively the linear and the nonlinear operators appearing in the model and $f(r,\theta)$ is the known analytic function. The solution of (4.1) can be expressed as

$$\widetilde{\psi}=\widetilde{\psi}_0+q\widetilde{\psi}_1+\ldots\ . \tag{4.2}$$

and therefore, the approximate solution of (4.1) can be readily obtained as

$$\psi=\lim_{q\to1}\widetilde{\psi}=\widetilde{\psi}_0+\widetilde{\psi}_1+\ldots\ . \tag{4.3}$$

Following a similar procedure the problem under consideration (3.6) can be written as

$$L(\widetilde{\psi})-L(\psi_0)+qL(\psi_0)+\frac{q}{ar}\left[\begin{array}{l}\frac{2b}{r}\frac{\partial^2}{\partial\theta\partial r}\Big\{r\Theta^m\Big(\frac{1}{r}\frac{\partial^2\widetilde{\psi}}{\partial\theta\partial r}-\frac{1}{r^2}\frac{\partial\widetilde{\psi}}{\partial\theta}\Big)\Big\}\\ +\frac{b}{r}\frac{\partial^2}{\partial\theta^2}\Big\{\Theta^m\Big(\frac{1}{r^2}\frac{\partial^2\psi}{\partial\theta^2}-\frac{\partial^2\psi}{\partial r^2}+\frac{1}{r}\frac{\partial\widetilde{\psi}}{\partial r}\Big)\Big\}\\ +\frac{2b}{r}\frac{\partial}{\partial\theta}\Big\{\Theta^m\Big(\frac{1}{r}\frac{\partial^2\widetilde{\psi}}{\partial\theta\partial r}-\frac{1}{r^2}\frac{\partial\widetilde{\psi}}{\partial\theta}\Big)\Big\}\\ -\frac{b}{r}\frac{\partial^2}{\partial r^2}\Big\{r^2\Theta^m\Big(\frac{1}{r^2}\frac{\partial^2\widetilde{\psi}}{\partial\theta^2}-\frac{\partial^2\psi}{\partial r^2}+\frac{1}{r}\frac{\partial\widetilde{\psi}}{\partial r}\Big)\Big\}\\ +\frac{b}{r^2}\frac{\partial^2}{\partial r^2}\Big\{r^2\Theta^m\Big(\frac{1}{r^2}\frac{\partial^2\widetilde{\psi}}{\partial\theta^2}-\frac{\partial^2\widetilde{\psi}}{\partial r^2}+\frac{1}{r}\frac{\partial\widetilde{\psi}}{\partial r}\Big)\Big\}\\ +2b\frac{\partial^2}{\partial\theta\partial r}\Big\{\Theta^m\Big(\frac{1}{r}\frac{\partial^2\widetilde{\psi}}{\partial\theta\partial r}-\frac{1}{r^2}\frac{\partial\widetilde{\psi}}{\partial\theta}\Big)\Big\}\end{array}\right]=0, \tag{4.4}$$

$$\Theta = 8\Big(\frac{1}{r}\frac{\partial^2\widetilde{\psi}}{\partial\theta\partial r} - \frac{1}{r^2}\frac{\partial\widetilde{\psi}}{\partial\theta}\Big)^2 + 2\Big(\frac{1}{r^2}\frac{\partial^2\widetilde{\psi}}{\partial\theta^2} - \frac{\partial^2\widetilde{\psi}}{\partial r^2} + \frac{1}{r}\frac{\partial\widetilde{\psi}}{\partial r}\Big)^2,$$

and where

$$L = \nabla^2\Big(\nabla^2\Big), \quad \nabla^2 = \frac{\partial^2}{\partial r^2} + \frac{1}{r}\frac{\partial}{\partial r} + \frac{1}{r^2}\frac{\partial^2}{\partial\theta^2}.$$

For the initial guess approximation, we take

$$\nabla^4\psi_0 = 0, \tag{4.5}$$

$$\frac{1}{r}\frac{\partial\psi_0}{\partial\theta} = U, \quad \frac{\partial\psi_0}{\partial r} = 0 \quad \text{at} \quad \theta = 0, \tag{4.6}$$

$$\frac{1}{r}\frac{\partial\psi_0}{\partial\theta} = 0, \quad \frac{\partial\psi_0}{\partial r} = 0 \quad \text{at} \quad \theta = \theta_0. \tag{4.7}$$

The solution of (4.5) together with boundary conditions (4.6) and (4.7), is given by $\psi_0 = UrF_0(\theta)$, where [24]

$$F_0(\theta) = \frac{\theta_0^2\sin\theta - \theta\sin\theta\Big(\theta_0 - \sin\theta_0\cos\theta_0\Big) - \theta\cos\theta\sin^2\theta_0}{\theta_0^2 - \sin^2\theta_0}. \tag{4.8}$$

Combining (4.2) and (4.4), and equating the coefficients of like powers of q on both sides, we get a system of equations which we consider in the following subsections.

Next we consider the zeroth and first oder systems.

4.1 Zeroth order system.

The first two linear equations in the system with their boundary conditions comprise the zeroth order problem and are given as

$$\nabla^4\Big(\widetilde{\psi_0}\Big) - \nabla^4\Big(\psi_0\Big) = 0, \tag{4.9}$$

$$\frac{1}{r}\frac{\partial\widetilde{\psi_0}}{\partial\theta} = U, \quad \frac{\partial\widetilde{\psi_0}}{\partial r} = 0 \quad \text{at} \quad \theta = 0, \tag{4.10}$$

$$\frac{1}{r}\frac{\partial\widetilde{\psi_0}}{\partial\theta} = 0, \quad \frac{\partial\widetilde{\psi_0}}{\partial r} = 0 \quad \text{at} \quad \theta = \theta_0. \tag{4.11}$$

The solution of (4.9) together with boundary conditions (4.10) and (4.11) is given by

$$\widetilde{\psi_0} = UrF_0(\theta),$$

where $F_0(\theta)$ is defined in (4.8).

4.2 First order system

The next set of equations that result comprise the 1st order system:

$$\nabla^4\Big(\widetilde{\psi}_1\Big)+\nabla^4\Big(\psi_0\Big)+\frac{1}{ar}\left[\begin{array}{l}\dfrac{2b}{r}\dfrac{\partial^2}{\partial\theta\partial r}\Big\{r\Phi^m\Big(\dfrac{1}{r}\dfrac{\partial^2\widetilde{\psi}_0}{\partial\theta\partial r}-\dfrac{1}{r^2}\dfrac{\partial\widetilde{\psi}_0}{\partial\theta}\Big)\Big\}\\ +\dfrac{b}{r}\dfrac{\partial^2}{\partial\theta^2}\Big\{\Phi^m\Big(\dfrac{1}{r^2}\dfrac{\partial^2\psi_0}{\partial\theta^2}-\dfrac{\partial^2\psi}{\partial r^2}+\dfrac{1}{r}\dfrac{\partial\widetilde{\psi}_0}{\partial r}\Big)\Big\}\\ +\dfrac{2b}{r}\dfrac{\partial}{\partial\theta}\Big\{\Phi^m\Big(\dfrac{1}{r}\dfrac{\partial^2\psi_0}{\partial\theta\partial r}-\dfrac{1}{r^2}\dfrac{\partial\widetilde{\psi}_0}{\partial\theta}\Big)\Big\}\\ -\dfrac{b}{r}\dfrac{\partial^2}{\partial r^2}\Big\{r^2\Phi^m\Big(\dfrac{1}{r^2}\dfrac{\partial^2\widetilde{\psi}_0}{\partial\theta^2}-\dfrac{\partial^2\widetilde{\psi}_0}{\partial r^2}+\dfrac{1}{r}\dfrac{\partial\widetilde{\psi}_0}{\partial\xi}\Big)\Big\}\\ +\dfrac{b}{r^2}\dfrac{\partial^2}{\partial r^2}\Big\{r^2\Phi^m\Big(\dfrac{1}{r^2}\dfrac{\partial^2\widetilde{\psi}_0}{\partial\theta^2}-\dfrac{\partial^2\widetilde{\psi}}{\partial r^2}+\dfrac{1}{r}\dfrac{\partial\psi_0}{\partial r}\Big)\Big\}\\ +2b\dfrac{\partial^2}{\partial\theta\partial r}\Big\{\Phi^m\Big(\dfrac{1}{r}\dfrac{\partial^2\psi_0}{\partial\theta\partial r}-\dfrac{1}{r^2}\dfrac{\partial\widetilde{\psi}_0}{\partial\theta}\Big)\Big\}\end{array}\right]=0, \tag{4.12}$$

where

$$\Phi=8\Big(\frac{1}{r}\frac{\partial^2\widetilde{\psi}_0}{\partial\theta\partial r}-\frac{1}{r^2}\frac{\partial\widetilde{\psi}_0}{\partial\theta}\Big)^2+2\Big(\frac{1}{r^2}\frac{\partial^2\widetilde{\psi}_0}{\partial\theta^2}-\frac{\partial^2\widetilde{\psi}_0}{\partial r^2}+\frac{1}{r}\frac{\partial\widetilde{\psi}_0}{\partial r}\Big)^2,$$

$$\frac{1}{r}\frac{\partial\widetilde{\psi}_1}{\partial\theta}=0,\quad \frac{\partial\widetilde{\psi}_1}{\partial r}=0\quad\text{at}\quad\theta=0,$$

$$\frac{1}{r}\frac{\partial\widetilde{\psi}_1}{\partial\theta}=0,\quad \frac{\partial\widetilde{\psi}_1}{\partial r}=0\quad\text{at}\quad\theta=\theta_0.$$

After substituting the zeroth order solution into (4.12), the resulting equation takes the form

$$\nabla^4\widetilde{\psi}_1=\frac{b}{a}\frac{2^m}{r^{2m+3}}\left\{\frac{d^2}{d\theta^2}\left(G^{2m+1}\right)-\left(4m^2-1\right)G^{2m+1}\right\}, \tag{4.13}$$

where $G=F_0+F_0''$, suggesting the solution of the form

$$\widetilde{\psi}_1=\frac{F_1}{r^{2m-1}}.$$

The partial differential equation (4.13) reduces to the following ordinary differential equation

$$F_1^{iv}+2(4m^2+1)F_1''+(4m^2-1)^2F_1=\frac{b}{a}\,2^mU^{2m+1}\times\left\{\frac{d^2}{d\theta^2}(G^{2m+1})-(4m^2-1)G^{2m+1}\right\}. \tag{4.14}$$

The corresponding boundary conditions are

$$F_1=0,\quad F_1'=0\quad\text{at}\quad\theta=0, \tag{4.15}$$

$$F_1=0,\quad F_1'=0\quad\text{at}\quad\theta=\theta_0. \tag{4.16}$$

It is not possible to attain the solution of (4.14) for a general m, we therefore discuss the following special cases.

4.2.1 The case with $m = 0$

For $m = 0$, (4.14) reduces to the form

$$F_1^{iv} + 2F_1'' + F_1 = 0,$$

which, together with the boundary conditions (4.15) and (4.16) gives the trivial solution.

4.2.2 The case with $m = 1$

For $m = 1$, (4.14) becomes

$$F_1^{iv} + 10F_1'' + 9F_1 = \frac{6b}{a}U^3 \left\{ \frac{d^2}{d\theta^2}\left(G^3\right) - 3G^3 \right\},$$

which, along with boundary conditions (4.15) and (4.16) gives the solution of the extended Taylor problem for a third grade fluid.

4.2.3 The case with $m = 2$

The final case we consider is for $m = 2$, where (4.14) takes the form

$$F_1^{iv} + 34F_1'' + 225F_1 = \frac{12b}{a}U^5 \Big\{ \frac{d^2}{d\theta^2}\left(G^5\right) - 15G^5 \Big\}. \tag{4.17}$$

The solution of (4.17) subjected to the boundary conditions (4.15) and (4.16) is given by

$$\begin{aligned} F_1 =& C_1 \cos 3\theta + C_2 \sin 3\theta + C_3 \cos 5\theta + C_4 \sin 5\theta \\ &+ \frac{12b}{a}U^5 \left\{ \begin{array}{l} E_{13}\cos\theta + E_{14}\theta \sin 3\theta + E_{15}\theta \sin 5\theta \\ +E_{16}\sin 3\theta + E_{17}\theta \cos 3\theta + E_{18}\theta \cos 5\theta \end{array} \right\}, \end{aligned} \tag{4.18}$$

where the C_i and E_i are constants depending upon θ_0 and are given by:

$$C_1 = -12U^5\frac{b}{a}E_{39},\ \ C_2 = 12U^5\frac{b}{a}E_{37},\ \ C_3 = 12U^5\frac{b}{a}E_{38},\ \ C_4 = -12U^5\frac{b}{a}E_{36},$$

$$d_1 = -\frac{2k}{\theta_0^2 - \sin^2\theta_0},\ \ d_2 = -\frac{2\sin^2\theta_0}{\theta_0^2 - \sin^2\theta_0},\ \ k = \theta_0 - \sin\theta_0\cos\theta_0,$$

$$E_1 = \frac{5d_1^5}{8} + \frac{10d_1^3d_2^2}{8} + \frac{5d_1d_2^4}{8},\quad E_2 = \frac{5d_1^5}{16} - \frac{10d_1^3d_2^2}{16} - \frac{15d_1d_2^4}{16},$$

$$E_3 = \frac{d_1^5}{16} - \frac{10d_1^3d_2^2}{16} + \frac{5d_1d_2^4}{16},\quad E_4 = \frac{5d_1^4d_2}{8} + \frac{10d_1^2d_2^3}{8} + \frac{5d_2^5}{8},$$

$$E_5 = \frac{-15d_1^4d_2}{16} + \frac{10d_1^2d_2^3}{16} - \frac{5d_2^5}{16},\ \ E_6 = \frac{5d_1^4d_2}{16} - \frac{10d_1^2d_2^3}{16} + \frac{d_2^5}{16},\ \ E_7 = -16E_1,$$

$$E_8 = -24E_2,\ \ E_9 = -40E_3,\ \ E_{10} = -16E_4,\ \ E_{11} = -24E_5,\ \ E_{12} = -40E_6,$$

$$E_{13} = \frac{1}{192}E_7,\ \ E_{14} = \frac{1}{96}E_8,\ \ E_{15} = -\frac{1}{160}E_9,\ \ E_{16} = \frac{1}{192}E_{10},$$

$$E_{17} = -\frac{1}{96}E_{11},\quad E_{18} = \frac{1}{160}E_{12},\quad E_{19} = E_{16} + E_{17} + E_{18},$$

$$E_{20} = -E_{13}\sin\theta_0 + E_{14}\sin 3\theta_0 + 3E_{14}\theta_0\cos 3\theta_0 + E_{15}\sin 5\theta_0 + 5E_{15}\theta_0\cos 5\theta_0 + E_{16}\cos\theta_0 + E_{17}\cos 3\theta_0 - 3E_{17}\theta_0\sin 3\theta_0 + E_{18}\cos 5\theta_0 - 5E_{18}\theta_0\sin 5\theta_0,$$

$$E_{21} = E_{13}\cos\theta_0 + E_{14}\theta_0\sin 3\theta_0 + E_{15}\theta_0\sin 5\theta_0 + E_{16}\sin\theta_0 + E_{17}\theta_0\cos 3\theta_0 + E_{18}\theta_0\cos 5\theta_0,$$

$$E_{22} = 3\sin 3\theta_0 - 5\sin 5\theta_0,\quad E_{23} = E_{20} + 3E_{13}\sin 3\theta_0,\quad E_{24} = \cos 5\theta_0 - \cos 3\theta_0,$$

$$E_{25} = E_{21} - E_{13}\cos 3\theta_0,\quad E_{26} = 3E_{24}\cos 3\theta_0,\quad E_{27} = 5E_{24}\cos 5\theta_0,$$

$$E_{28} = E_{23}E_{24},\quad E_{29} = E_{22}\sin 3\theta_0,\quad E_{30} = E_{28}\sin 5\theta_0,\quad E_{31} = E_{22}E_{25},$$

$$E_{32} = E_{26} - E_{29},\quad E_{33} = E_{27} - E_{30},\quad E_{34} = E_{28} - E_{31},\quad E_{35} = 5E_{32} - 3E_{33},$$

$$E_{36} = E_{19}E_{32} - 3E_{34},\quad E_{37} = \frac{E_{36}}{E_{35}},\quad E_{38} = \frac{E_{33}E_{37} - E_{34}}{E_{32}},$$

$$E_{39} = \frac{E_{30}E_{37} - E_{38}E_{29} - E_{31}}{E_{22}E_{24}},\quad E_{40} = E_{39} + E_{13}.$$

Combining the expressions for $\widetilde{\psi}_0$ and $\widetilde{\psi}_1$, the solution of the problem under discussion after making use of (4.3) is given by

$$\psi = UrF_0 + \frac{F_1}{r^3}, \tag{4.19}$$

where F_0 and F_1 are respectively given by (4.8) and (4.18). Using (3.5), the velocity components u and v are obtained as

$$u = UF_0' + \frac{F_1'}{r^4},\quad v = -UF_0 + \frac{3F_1}{r^4}.$$

In order to discuss the forces acting on the scraper, we devote the next section to the determination of the normal and shear stresses.

5 Normal and Shear Stresses

We start by noting that the pressure distribution for this problem is given by

$$p = -\frac{a}{r}UG' - \frac{a}{5r^5}\left(9F_1' + F_1'''\right) - \frac{12b}{5r^5}U^5\frac{d}{d\theta}\left(G^5\right).$$

Substituting the expressions for pressure field, extra stress tensors and then writing the Cauchy stress tensor in component form, the normal and the shear stresses are given as

$$\mathbf{T}_{\theta\theta} = \frac{aU}{r}G' + \frac{aU^3}{30r^5}\left(F_1''' + 49F_1'\right) + \frac{12b}{5r^5}\frac{d}{d\theta}\left(G^5\right),$$

$$\mathbf{T}_{r\theta} = \frac{aU}{r}G + \frac{aU^3}{6r^5}\left(F_1'' - 15F_1\right) + \frac{12b}{r^5}G^5.$$

Let us denote respectively by T_n and T_t the normal and tangential stresses to the scraper (*i.e* for $\theta = \theta_0$) at a distance r from the point of contact. Then the component L of the total stress perpendicular to the plate is given by

$$L = T_n \cos\theta_0 + T_t \sin\theta_0.$$

Similarly, the component D parallel to the plate is

$$D = T_n \sin\theta_0 - T_t \cos\theta_0.$$

Now, we construct tables of values for both viscous fluid and Sisko fluid flows and see the effects of T_n, T_t, L and D by giving different values to angle θ_0.

Table 1. Values of L, D, T_n, and T_t divided by $2\mu U/r$ for various values of θ_0 for a viscous fluid.

θ_o	$T_n r/2\mu U$	$T_t r/2\mu U$	$Lr/2\mu U$	$Dr/2\mu U$
0	∞	∞	∞	∞
15	43	3.82	42	7.5
30	10.8	2.03	10.3	3.67
45	4.8	1.31	4.30	2.44
60	2.61	0.98	2.15	1.77
75	1.61	0.80	1.19	1.36
90	1.07	0.68	0.68	1.07
105	0.73	0.60	0.38	0.85
120	0.50	0.53	0.21	0.70
135	0.33	0.47	0.10	0.56
150	0.20	0.42	0.04	0.46
165	0.08	0.37	0.01	0.38
180	0	0.32	0	0.32

Table 2. Values of L, D, T_n, and T_t divided by $2\mu U/r$ for a various values of θ_0 for a Sisko fluid.

θ_o	$T_n r/2\mu U$	$T_t r/2\mu U$	$Lr/2\mu U$	$Dr/2\mu U$
0	∞	∞	∞	∞
15	6.38×10^{17}	4.16×10^{18}	4.60×10^{17}	-4.18×10^{10}
30	8.06×10^{10}	9.51×10^{10}	1.17×10^{11}	-4.20×10^{18}
45	∞	∞	∞	∞
60	79811	329857	244802	-235704
75	8304.75	8775.77	6193	-10794
90	∞	∞	∞	∞
105	-54.71	99.09	99.60	11.18
120	-36.54	-177.15	-157	82.35
135	∞	∞	∞	∞
150	-13.67	-29.75	-22.65	21.27
165	-391.55	-26.87	-31.871	26.79
180	∞	∞	∞	∞

We now look at various values of L, D, T_n, and $T_t/2\mu U/r$ for various values of θ_0 for both viscous and Sisko fluid flows, these values are given in Tables 1, 2. It can be seen that D decreases as θ_0 increases for viscous flow and it attains its least positive value at $\theta_0 = \pi$, but for Sisko fluid flow D

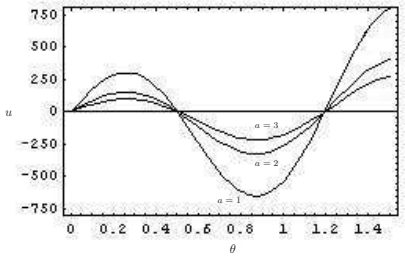

Figure 2. Variation of velocity component u versus the parameter a. For computing this graph $r = 1.5, U = 0.8, b = 2$ and $\theta_o = 4\pi/9$.

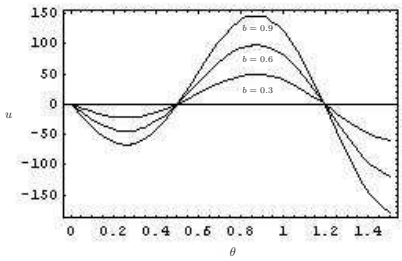

Figure 3. Variation of velocity component u versus the parameter b. For computing this graph $r = 1.5, U = 0.8, a = 2$ and $\theta_o = 4\pi/9$.

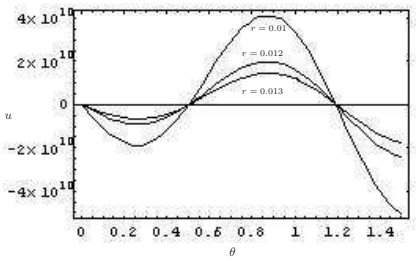

Figure 4. Variation of velocity component u versus the radial distance r. For computing this graph $b = 0.5, U = 0.8, a = 2$ and $\theta_o = 4\pi/9$.

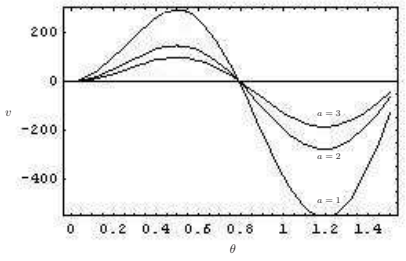

Figure 5. Variation of velocity component v versus the parameter a. For computing this graph $r = 1.5, U = 0.8, b = 2$ and $\theta_o = 4\pi/9$.

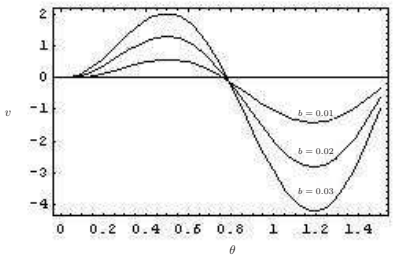

Figure 6. Variation of velocity component v versus the parameter b. For computing this graph $r = 1.5, U = 0.8, a = 2$ and $\theta_o = 4\pi/9$.

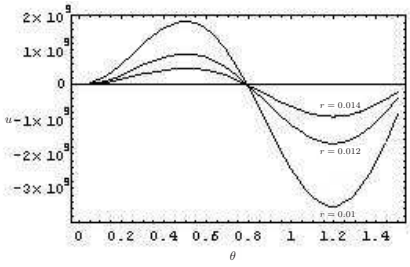

Figure 7. Variation of velocity component v versus the radial distance r. For computing this graph $b = 0.05, U = 0.8, a = 2$ and $\theta_o = 4\pi/9$.

remains negative in the range $0 < \theta_0 < 5\pi/12$ and then it increases in the range $5\pi/12 < \theta_0 < \pi$. For viscous flow, the most interesting and perhaps unexpected feature of the calculations is that L does not change sign in the range $0 < \theta_0 < \pi$. But for Sisko fluid flow the case is different, here L changes sign in the range $2\pi/3 < \theta_0 < \pi$. By this comparison, we note that for Sisko fluid flow we have to keep the angle θ_0 larger as compared to the viscous fluid flow to scrape the fluid easily. We further see that for viscous fluid flow there

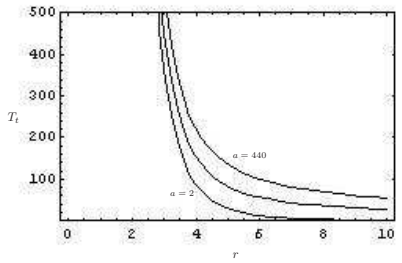

Figure 8. Variation of tangential stress T_t versus the parameter a. For computing this graph $b = 5, U = -0.8$ and $\theta_o = 4\pi/9$.

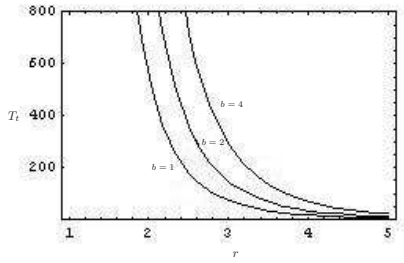

Figure 9. Variation of tangential stress T_t versus the parameter b. For computing this graph $a = 0.05, U = 0.8$ and $\theta_o = 4\pi/9$.

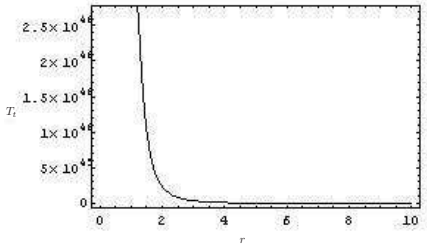

Figure 10. Variation of tangential stress T_t versus the parameter $\theta_o = 0.01$ radians. For computing this graph $b = 5, U = -0.8$ and $a = 4$.

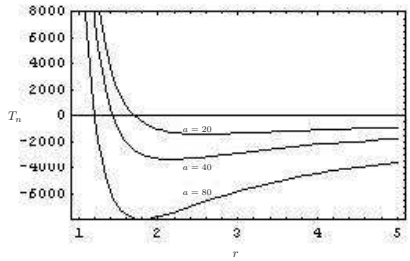

Figure 11. Variation of tangential stress T_n versus the parameter a. For computing this graph $b = 4, U = 0.8$ and $\theta_o = 4\pi/9$.

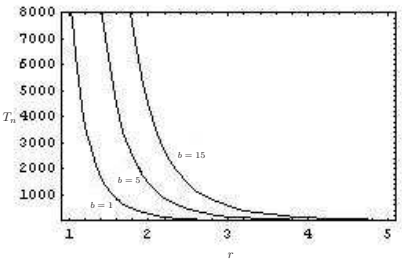

Figure 12. Variation of normal stress T_n versus the parameter b. For computing this graph $a = 40, U = 0.8$ and $\theta_o = 4\pi/9$.

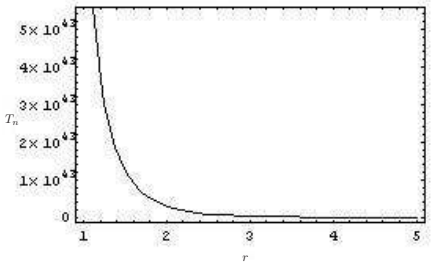

Figure 13. Variation of normal stress T_n versus $\theta_0 = 0.01$ radians. For computing this graph $a = 40, U = 0.8$ and $b = 15$.

occurred only one singularity at $\theta_0 = 0$ in the stress field, but for Sisko fluid flow, we have five such points *i.e* at $\theta_0 = 0$, $\pi/4$ $\pi/2$, $3\pi/4$, π. This means that holding the scraper at these positions, we cannot scrape the fluid for Sisko fluid flow or there will be an infinite force required to scrape the fluid.

6 Discussion

In this section we present some graphs to show the behavior of the velocity field, tangential and normal stresses and the stream function. In Figures 2–4,

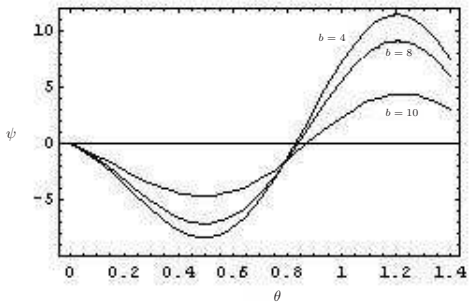

Figure 14. Stream function against the parameter b. For computing this graph $a = 4, U = -0.8, r = 10$ and $\theta_o = 4\pi/9$.

the velocity component u is sketched against certain parameters for fixed values of other parameters. In Fig. 2 it is seen that initially for small values of angle θ, u decreases in the positive direction but at the later stage reverse flow occurs and u increases as a increases in the interval $\theta \in (0.4, 1.4)$. It is worth noting that the absolute value of u always decreases as a increases. In Fig. 3 we notice a slightly different trend in that u starts decreasing in the negative direction, but latter, *i.e.,* $\theta \in (0.4, 1.4)$ we see that u increases with the parameter b; the velocity changes are smaller than the changes against the parameter a. In Fig. 4 we have tried to show the velocity trend against the radial distance r, it is observed that near the corner, the velocity increases rapidly, reflecting the presence of a corner singularity in the flow field. In Figs. 5–7, the velocity component v is sketched against the same parameters. Similarly, in Fig. 5 we see how v behaves against a, but the magnitude of v is much smaller than that of u, although the circumstances are the same. In Fig.6 it can be noted that v increases as b increases. In Fig.7 the component v has been exposed near the corner and it is observed that it becomes singular at the corner. Fig.8 demonstrates the behavior of the tangential stress versus the parameter a, the values of the other parameters are fixed. It can be seen that stress increases with a, but near the corner it also becomes singular. Also, from Fig.9 we note that the stress is proportional to the parameter b. From the mathematical analysis in the previous section, we realize, that the whole flow field is singular at $\theta_0 = 0$; Figs.10 and 13 are the justification of this fact as for $\theta_0 = 0.01$. We note that stresses increase very rapidly and the same happens in the case for other flow quantities (velocity etc.). In Fig.11 and 12, we see that the normal stress always decreases against the parameter a. It should be noted that both the normal and tangential stresses are calculated for the upper plane (scraper). Finally, Fig.14 depicts the stream function ψ, pattern of flow of a Sisko fluid near the wedge of two intersecting planes versus the parameter b.

7 Conclusion

The flow of a Sisko fluid near the corner of two intersecting rigid planes has been analyzed. The non-linear partial differential equations modeling the flow are

solved to obtain the expressions for the stress field, velocity field and pressure field. It is noted that, if we set $b = 0$ in the constitutive equation for the Sisko model [23], on one side, we get the Newtonian model, and on the other side, the substitution of the constant $b = 0$ in the solution (4.19), gives the Taylor's solution of the well known paint-scraper problem [24]. This is a reasonable verification of the problem.

References

[1] S. Abbasbandy. Application of He's homotopy perturbation method for Laplace transform. *Chaos, Solitons & Fractals*, **30**(5):1206, 2006. (doi:10.1016/j.chaos.2005.08.178)

[2] William J. Bailey and Iain S. Weir. Investigation of methods for direct rheological model parameter estimation. *Journal of Petroleum Science and Engineering*, **21**:1–13, 1998. (doi:10.1016/S0920-4105(98)00040-0)

[3] G.K. Batchelor. *An introduction to fluid dynamics*. Cambridge University Press, 1967.

[4] R.K. Bhatnagar, K.R. Rajagopal and G. Gupta. Flow of an oldroyd-B fluid between intersecting planes. *Journal of non-Newtonian Fluid Mechanics*, **46**:49–67, 1993. (doi:10.1016/0377-0257(93)80003-T)

[5] R.B. Bird, R.C. Armstrong and O. Hassager. *Dynamics of polymeric liquids*, volume 1. John Wiley & Sons, New York, 1987.

[6] L. Cveticanin. Homotopy perturbation method for pure nonlinear differential equation. *Chaos, Solitons & Fractals*, **30**(5):1221–1230, 2006. (doi:10.1016/j.chaos.2005.08.180)

[7] M. El-Shahed. Application of He's homotopy perturbation method for Laplace transform. *International Journal of Nonlinear Science Numerical Simulation*, **6**:163, 2005.

[8] I.H. Gucuyener. An evalution of the rheological models describing drilling fluids and cement slurries. In *Proceedings of the 9th Petroleum Congress of Turkey UCTEA Chamber of geophysical engineers*, Ankara, Turkey, February, 1992.

[9] J.H. He. Homotopy perturbation technique. *Computer Methods in Applied Mechanics and Engineering*, **178**:257–262, 1999.

[10] J.H. He. New interpretation of homotopy perturbation method. *International Journal of Modern Physics B*, **20**(18):2561–2568, 2006.

[11] A.M. Hull. An exact solution for the slow flow of a general linear viscoelastic fluid through a slit. *Journal of non-Newtonian Fluid Mechanics*, **8**:327–336, 1981. (doi:10.1016/0377-0257(81)80029-8)

[12] P.N. Kaloni and M.T. Kamel. A note on the hamel flow of cosserat fluids. *ZAMP*, **31**:293–296, 1980. (doi:10.1007/BF01590754)

[13] M. Khan, S. Hyder Ali and Haitao Qi. Exact solutions of starting flows for a fractional burgers fluid between coaxial cylinders. *Nonlinear Analysis: Real World Applications*, **10**(3):1775–1783, 2009. (doi:10.1016/j.nonrwa.2008.02.015)

[14] A. Kolyshkin and S. Nazarovs. Stability of slowly diverging flows in shallow water. *Math. Model. Anal.*, **12**(1):101–106, 2007. (doi:10.3846/1392-6292.2007.12.101-106)

[15] A. Krylovas and R. Čiegis. Asymptotical analysis of one dimensional gas dynamics equations. *Math. Model. Anal.*, **6**(1):117–128, 2001.

[16] D.C. Kuzma, E.R. Maki and R.J. Donnelly. The magnetohydrodynamic squeeze film. *Journal of Tribology*, **110**:375–377, 1988.

[17] D. Mansutti and K.R. Rajagopal. Flow of shear thinning fluid between intersecting planes. *International Journal of Nonlinear Mechanics*, **26**:769–775, 1991. (doi:10.1016/0020-7462(91)90027-Q)

[18] V. Marinca, N. Herisanu, C. Bota and B. Marinca. An optimal homotopy asymptotic method applied to the steady flow of a fourth-grade fluid past a porous plate. *Applied Mathematics Letters*, **22**:245–251, 2009. (doi:10.1016/j.aml.2008.03.019)

[19] H.K. Moffat. Viscous and resistive eddies near a sharp corner. *Journal of Fluid Mechanics*, **18**:1–8, 1964. (doi:10.1017/S0022112064000015)

[20] A.H. Nayfeh. *Introduction to Perturbation Techniques*. John Wiley & Sons, New York; Chichester, 1981.

[21] A.M. Siddiqui, M. Ahmed and Q.K. Ghori. Couette and Poiseuille flow for non-Newtonian fluids. *International Journal of Nonlinear Sciences and Numerical Simulation*, **7**(1):15–26, 2006.

[22] A.M. Siddiqui, R. Mahmood and Q.K. Ghori. Thin film flow of a third grade on a moving belt by He's homotopy perturbation method. *International Journal of Nonlinear Sciences and Numerical Simulation*, **7**(1):7–14, 2006.

[23] A.W. Sisko. The flow of lubricating greases. *Industrial and Engineering Chemistry Research*, **50**(12):1789–1792, 1958.

[24] G.I. Taylor. On scraping viscous fluid from a plane surface. In G.K. Batchelor(Ed.), *The scientific Papers of Sir Geoffrey Ingram Taylor*, pp. 410–413, 1971.

[25] J. Xu. *Rheology of polymeric suspensions: Polymer nanocomposites and waterborne coatings*. Industrial and Engineering Chemistry coatings, PhD thesis, Ohio State University, 2005.